Int. J. Electrochem. Sci., 15 **(2020)** 5860 – 5877, doi: 10.20964/2020.06.56

International Journal of
ELECTROCHEMICAL
SCIENCE
www.electrochemsci.org

Voltammetric analysis of Dopamine in the Presence of Large Concentration of Ascorbic Acid at Nickel Oxide-Gold Nanoparticles Binary Electrocatalyst

Zahrah T. Al-thagafi[1,2], *M. I. Awad*[1,3,*]

[1] Chem. Department, Faculty of Applied Sciences, Umm Al-Qura University, Makkah, Saudi Arabia.
[2] Chem. Department, Faculty of Sciences, Taif University, Taif, Saudi Arabia.
[3] Chem. Department, Faculty of Science, Cairo University, Cairo, Egypt.
[*]E-mail: mawad70@yahoo.com

Received: 1 February 2020 / *Accepted:* 24 March 2020 / *Published:* 10 May 2020

The current investigation presents electrodeposition of nickel oxide (nano-NiO_x) and gold nanoparticles (AuNPs) onto glassy carbon electrode (GC/NiO_x-Au), and the subsequent application of this electrode for the analysis of dopamine (DA) in the presence of excess concentration of ascorbic acid (AA). Based on its catalytic function towards the oxidation of DA and AA, the overlapping voltammetric response of the DA and AA at the bare electrode is resolved into two well-defined voltammetric peaks with lowered oxidation potential and enhanced oxidation currents. The sequence of deposition sequence of nano-NiO_x and AuNPs was adjusted for tuning the electrocatalytic activity and sensitivity. The highest catalytic activity and sensitivity towards the two species was obtained at the electrode modified by NiO_x and then AuNPs. Also, the modified electrode has been electrochemically and morphologically characterized using SEM, EDX and XRD. The practical analytical utility of the electrode is illustrated by the simultaneous determination of DA and AA in real samples (commercially available pharmaceutical formulation) without any preliminary treatment**.**

Keywords: Electrocatalysis, Gold nanoparticles, Nickel oxide nanoparticles, Glassy carbon electrode, Dopamine, Ascorbic acid

1. INTRODUCTION

DA and AA play an important role in the human body. DA, 2-(3,4dihydroxyphenyl)-ethylamine, is a chemical neurotransmitter in particular structures of the brain and plays a crucial role in the function of central nervous, hormonal, renal and cardiovascular systems [1]. Deficiency of DA are related to several diseases such as Parkinson's disease and schizophrenia [2, 3]. Therefore, the DA concentration determination in body fluids is of great significance in the diagnostics of such diseases. A major problem

for the detection of DA is the co-existence of many interfering compounds in biological systems. The typical concentration of DA is around one to thousand-fold of AA, which is a cofactor of multiple enzymes [4,5].

Ascorbic acid (vitamin C) is an important biological component of living beings. It is required for building intercellular substances, regenerating and healing tissues, maintaining vascular integrity, and providing a normal haematological and immunological status of the body and its resistance against infections and stresses. AA takes part in many biocatalytic reactions [6]. To quantify DA coexisting with a large excess of AA, the major challenge is to achieve both high selectivity and sensitivity of the detection technique.

The development of rapid and simple methods for determining DA and AA in biological fluids is of doubtless interest. In literature, titrimetry [7], spectrophotometry [8], chemiluminescence [9] and high-performance liquid chromatography (HPLC) [10] have been used for DAA and AA analysis. However, these methods have some limitations. A low sensitivity is a drawback of spectrophotometry and titrimetry. HPLC demands a preliminary sample preparation that sometimes involves a derivatization stage [11]. Electrochemical methods ensure a high rapidity, sensitivity, and selectivity of determining a number of biologically active substances.

Determination of DA in human body fluids using electrochemical techniques is interfered with the coexisting excess AA [12]. At standard electrodes, DA and AA are electrochemically oxidixed at potentials close to each other. This results in overlapping voltammetric response of both species. To solve this problem, various chemically modified electrodes have been used aiming at increasing the sensitivity, thus improving the selectivity, especially for DA in the presence of excess of AA. These electrodes include ruthenium oxide modified electrode [13], AuNPs distributed poly(4-aminothiophenol) modified electrode [14], Fe_3O_4 nanoparticles modified electrode [15], poly(4-(2-pyridylazo)-resorcinol) modified glassy carbon electrode [16] and nickel(II) complex polymer-modified electrodes [17]. However, this issue needs further research to imporve the selectivity, especially in the case of analyzing both species wheare AA concentration is much larger than DA.

In recent years, advances in bioelectrochemistry have centred on investigations of nanomaterials. Among a variety of nanomaterials, AuNPs, are one of the most attractive due to their interesting properties arising from larger active surface area and improved electron transport in biosensor studies [18,19]. Metal oxide nanoparticles as a nanomaterial have great attention due to their optical, magnetic, and electronic properties [20]. Among them, nano-NiO_x is a promising material for the development of biosensors due to its high chemical stability, high electron transfer properties, high electrocatalytic properties, nontoxicity, and biocompatibility [21]. It is reported that nano-NiO_x modified electrodes exhibited high electrocatalytic activity toward different biological materials [22-24]. The present work investigates nano-NiO_x/AuNPs fabricated GC electrode for DA analysis in the presence of excess of AA at physiological pH. The modified electrode presented high selectivity as well as senstivity. Then, the modified electrode was applied for the determination of DA and AA in real samples (pharmaceutical formulations).

2. EXPERIMENTAL

2.1. Chemicals and solutions.

All chemicals /reagents were of analytical grade and used without further purification. Deionized water was used to prepare all the aqueous solutions. Freshly prepared solution of dopamine hydrochloride (DA) and AA were used in all experiments. DA and AA were purchased from Sigma Chemical Co. (USA). Phosphate buffer solution (PBs) of pH=7.0 was used as the supporting electrolyte. The pH was adjusted to appropriate values with concentrated solutions of NaOH and H_2SO_4.

2.2. Apparatus and Electrodes.

All the electrochemical experiments were carried out using Gamry Instrument (Potentiostat/galvanostat/ZRA model the Reference 600 ™). A conventional three electrodes system with a platinum wire as an auxiliary electrode, modified GC electrode (GC/NiO_x-Au) was used as working electrode and saturated calomel electrode (SCE) as reference electrode. The GC electrode (1 mm in diameter) was polished to a mirror shine using polishing papers of two grades (3000 and 2000) and cleaned thoroughly with deionized water successively. The pH of the buffers was measured using Hanna Instruments HI 2213 pH Meter using a combination glass electrode.

2.3. Electrode Modification.

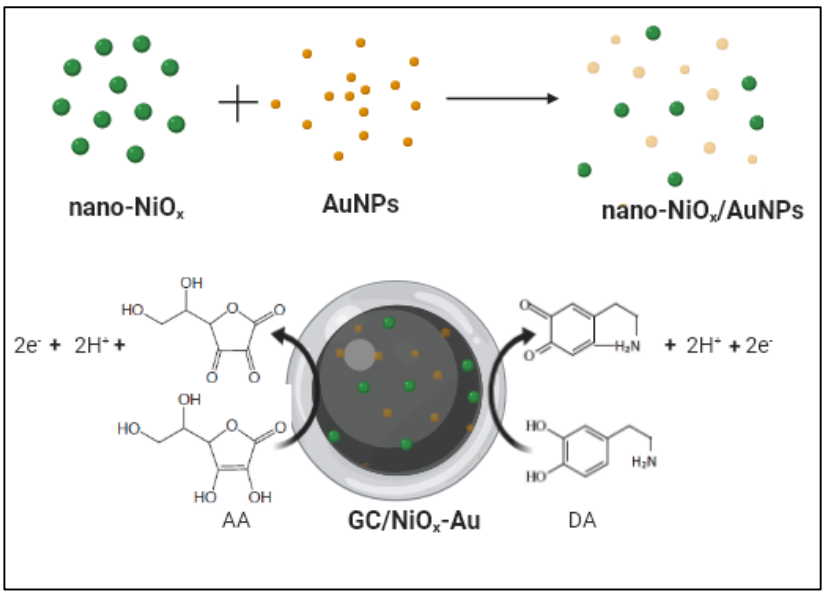

Scheme 1. Steps of Fabrication of (GC/ NiO_x-Au) electrode

GC electrode modification with (nano-NiO_x and AuNPs) was achieved in two sequential steps. The first involved the deposition of nano-NiO_x on GC by Electrodeposition from Watts bath [25]; (0.02 M $NiSO_4 \cdot 6H_2O$ + 0.03 M $NiCl_2 \cdot 6H_2O$ + 0.03 M H_3BO_3) by cycling the potential in the range 0 to –

1.0 V vs. SCE at a scan rate 50 mv s^{-1}, temperature = 25 ºC. Then the electrode was subjected to several potential cycles between 0 and 0.7 V vs. (SCE) in 0.5 M NaOH for oxidizing the thus deposited nickel. Next, the electrodeposition of AuNPs was carried from 0.5 M H_2SO_4 solution containing 1.0 mM Na $[AuCl_4].2H_2O$ solution using CV by potential cycling from 1.0 to 0 V vs. SCE for 10 cycles (see Scheme 1).

2.4. Instrumentation.

The morphology and composition of the modified electrode were studied by scanning electron microscopy (SEM, JSM-7600F Field Emissions Scanning Electron Microscope), equipped with energy dispersive spectroscopy (EDX, Inca Oxford Instrument). The crystallographic structure of nano-NiO_x/AuNPs was inspected using X-Ray Diffraction (XRD, D8 Discover Bruker using 2 theta from 5-90 degree with 2 degree per minute scan speed).

3. RESULTS AND DISCUSSION

3.1. Modified electrode characterization.

The morphology of the modified electrodes were analyzed by SEM. Fig. 1 shows typical SEM images of the bare GC, GC/AuNPs, GC/nano-NiOx, GC/Au-NiOx (AuNPs deposited first followed by nano-NiOx) and GC/NiOx-Au (nano-NiOx deposited first followed by AuNPs) electrodes. Significant differences in the surface morphology of electrodes are observed. As it can be seen in (Fig.1a), the bare GC electrode is smooth. In (Fig. 1b), AuNPs of uniform distribution are electrodeposited onto bare GC. On the other hand, the nano-NiOx were deposited onto the GC surface in a flower-shaped geometry (Fig. 1c). At the GC/Au-NiOx electrode (Fig. 1d), a small increase in particle size and a slightly higher filling density of the pores. In image (Fig. 1e), a uniform distribution of the binary catalyst is obtained.

The EDX analysis was conducted to inspect the elemental composition of the different electrodes (Fig. 2) and extracted data from this figure are represented in Table 1. As can be seen in Fig.2, the GC/AuNPs (Fig. 2b) exhibits smaller gold signal, at 2.12 keV on the expense of the decrease of carbon peak at 0.27 keV, as compared with the bare GC (Fig. 2a). For GC/nano-NiO_x electrode (Fig. 2c) the nickel signal appeared, also the oxygen signal increased in weight % compared with the bare GC (Fig. 2a), that evidence of the deposition of nano-NiO_x onto GC. The prominence of nickel, oxygen and gold peaks in the EDX spectra at GC/Au-NiO_x electrode (Fig. 2d) confirm the successful depositions of nano-NiO_x and AuNPs on GC electrode. Interestingly, for GC/NiO_x-Au electrode (Fig. 2e), the peaks of nickel, oxygen and gold peaks are larger, while that of the carbon is the smallest compared with other studied electrodes.

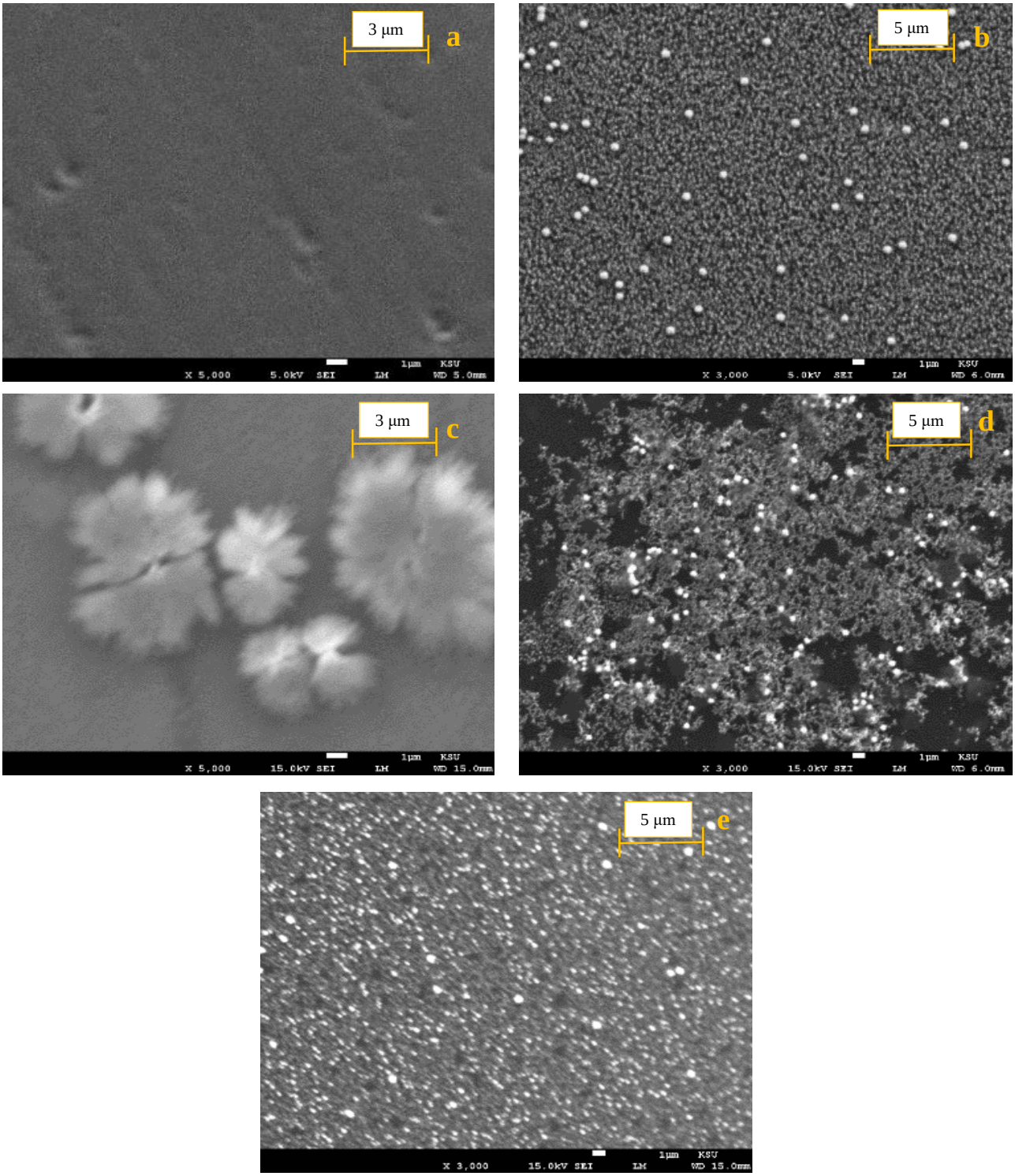

Figure 1. SEM images of (a) Bare GC, (b) GC/AuNPs, (c) GC/nano-NiO_x, (d) GC/Au-NiO_x and (e) GC/NiO_x-Au electrodes.

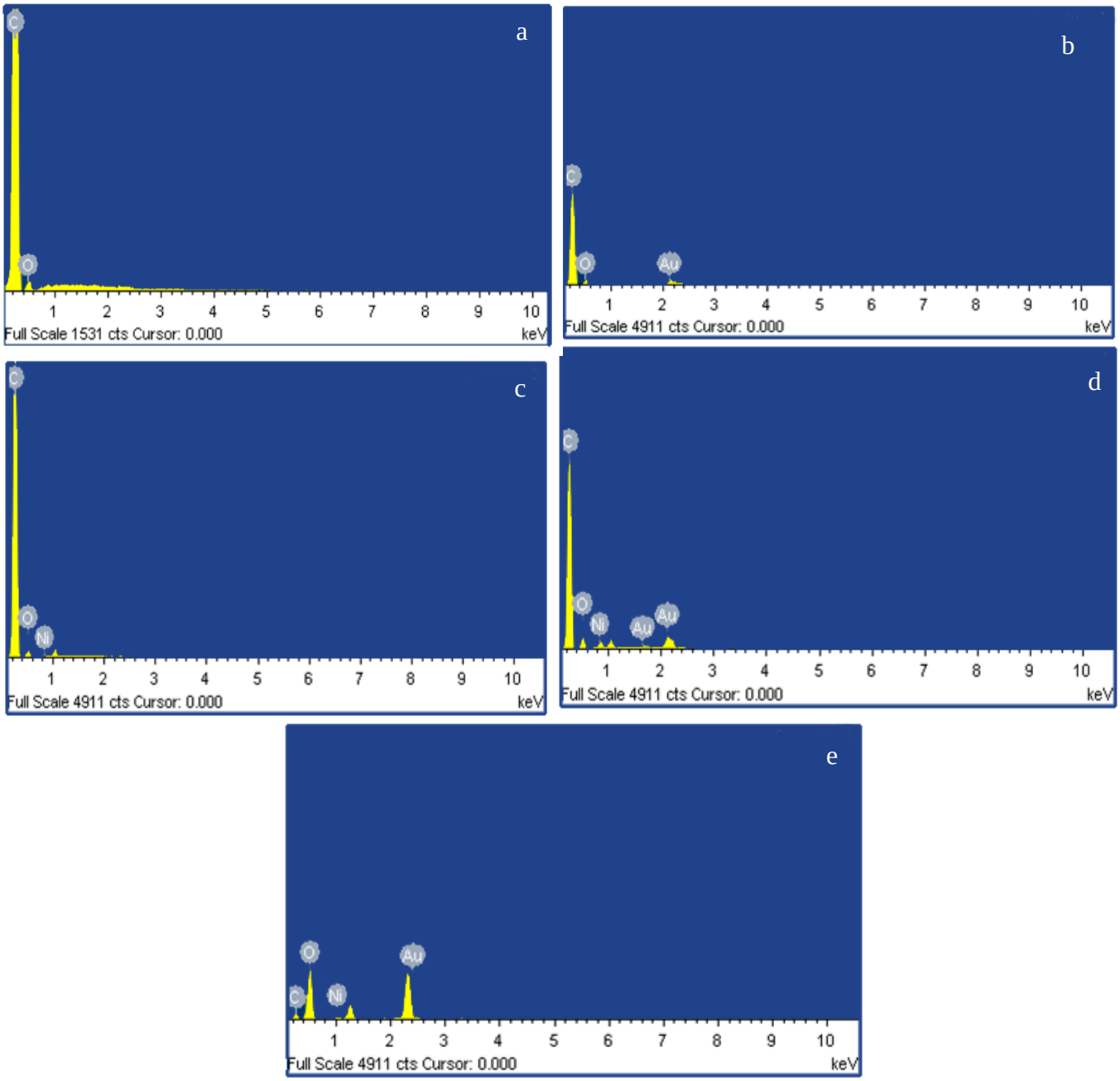

Figure 2. EDX analysis of (a) Bare GC, (b) GC/AuNPs, (c) GC/nano-NiO_x, (d) GC/Au-NiO_x and (e) GC/NiO_x-Au electrodes.

Table 1. EDX analysis of GC, GC/AuNPs, GC/nano-NiO_x, GC/Au-NiO_x and GC/NiO_x-Au electrodes

Electrode	Elements	Atomic content, at., %	Weight content, wt., %
GC	C K	97.65	96.89
	O K	2.35	3.11
GC/AuNPs	C K	90.87	83.67
	O K	8.77	10.75

	Au K	0.37	5.58
GC/nano-NiO$_x$	C K	94.27	92.17
	O K	5.08	6.62
	Ni K	0.64	1.21
GC/Au-NiO$_x$	C K	89.43	78.27
	O K	9.43	10.99
	Ni K	0.55	2.37
	Au K	0.58	8.37
GC/NiO$_x$-Au	C K	20.31	14.21
	O K	62.46	56.50
	Ni K	4.44	6.07
	Au K	12.80	23.21

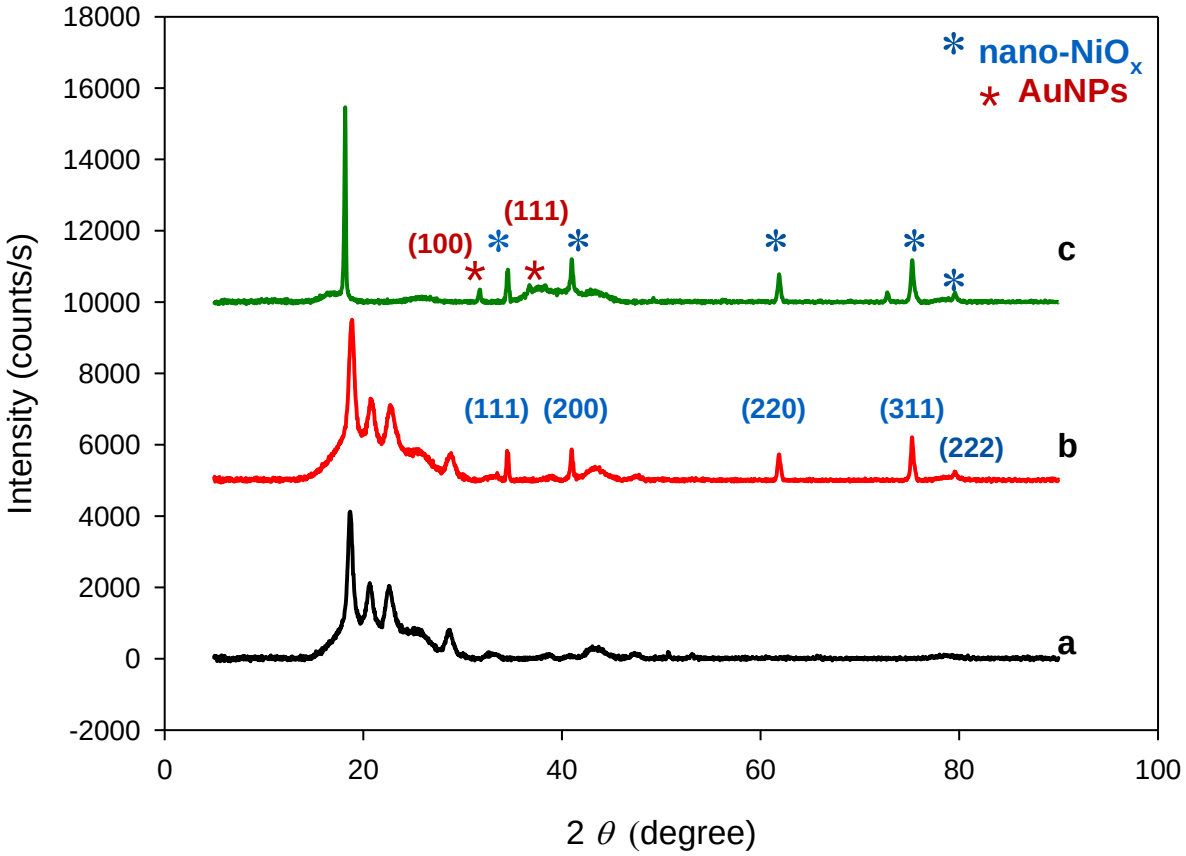

Figure 3. XRD analysis of (a) Bare GC, (b) GC/nano-NiO$_x$ and (c) GC/NiO$_x$-Au electrodes.

The XRD patterns of bare GC, GC/nano-NiO$_x$ and GC/NiO$_x$-Au electrodes are shown in Fig.3. The bare GC electrode in (Fig.3a) shows a broad, amorphous diffraction peak at approximately about 2 theta = 19° which corresponds to the (002) diffraction of the carbon substrate [26]. For GC/nano-NiO$_x$ electrode (Fig.3b), the diffraction peaks at 2 theta values of 34.91°, 41.27°, 61.99°, 75.12° and 79.35° corresponds to (111), (200), (220), (311), and (222) crystal planes, respectively, which indicated the formation of cubic crystalline NiO$_x$ [27,28]. In (Fig.3c), along with some predominant peaks of NiO$_x$,

one can see the presence of additional diffraction peaks located at about 31.72° and 38.00° which can be indexed as the (100) and (111) planes of Au nanoparticles [29]. This indicates the successful formation GC/NiO_x-Au onto GC electrode.

3.2. Electrochemical characterization.

Fig. 4 shows CVs obtained at (a, b) bare GC, (c) GC/AuNPs, (d) GC/nano-NiO_x, (e) GC/Au-NiO_x and (f) GC/NiO_x-Au electrodes in PBs (pH 7.0) (a) containing 0.25 mM DA + 1.0 mM AA (b-f). GC/NiO_x-Au was prepared using 2 potential cycles of Ni and 10 potential cycles of Au (optimum) at a scan rate 100 mV s^{-1}. Bare GC (b) electrode failed to separate the oxidation peaks of AA and DA. However, GC/AuNPs, GC/nano-NiO_x, GC/Au-NiO_x and GC/NiO_x-Au electrodes resolves the oxidation peaks of AA and DA, where oxidation of DA occurs at ~159 mV and the oxidation of AA occurs at ~ -20 mV vs. SCE. The larger separation of peak potential of DA and AA is obtained at GC/NiO_x-Au electrode (curve f).

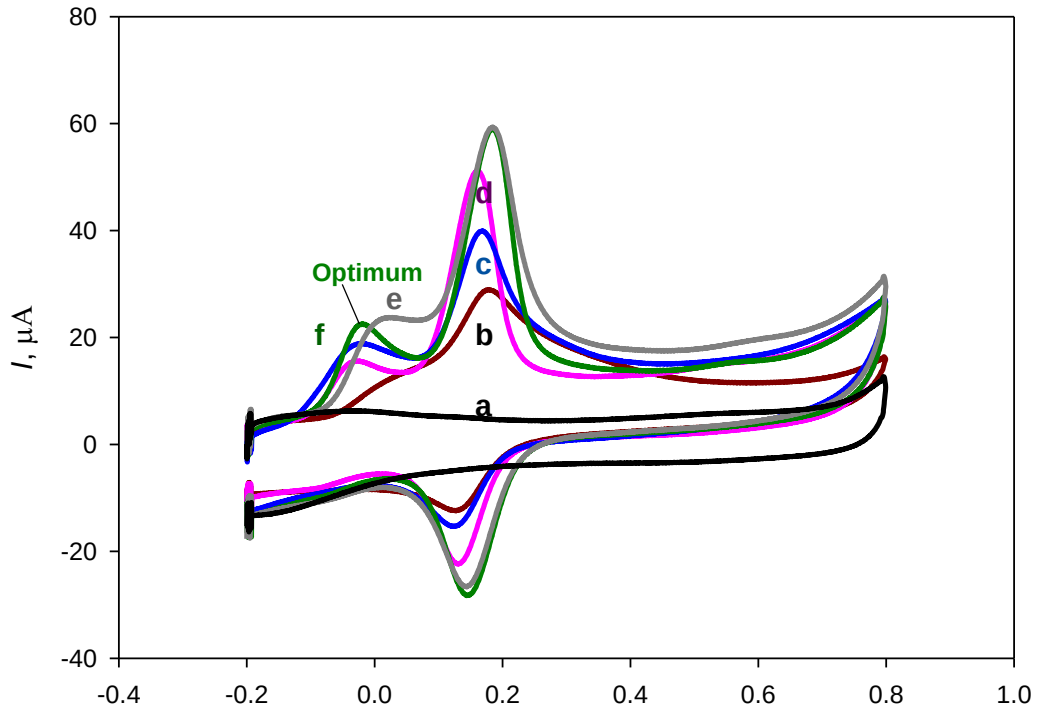

Figure 4. CVs obtained at (a, b) bare GC, (c) GC/AuNPs, (d) GC/nano-NiO_x, (e) GC/Au-NiO_x and (f) GC/NiO_x-Au electrodes in PBs (pH 7.0) (a) containing 0.25 mM DA + 1.0 mM AA (b-f). GC/NiO_x-Au was prepared using 2 potential cycles for Ni deposition and 10 potential cycles for deposition of Au (optimum). Scan rate 100 mV s^{-1}.

3.3. Effect of pH.

The choice of the type of the supporting electrolyte and its pH is critical in electroanalysis because they affect the properties of the solution as well as the electrode–solution interface, modifying the

thermodynamics and kinetics of the charge transfer process, and the adsorption at the electrode surface [30]. Effect of pH of the supporting electrolyte (PBs) on the oxidation of DA and AA at GC/NiO_x-Au was studied and shown in Fig. 5. The anodic peak potential for DA and AA are well separated over studied pH range, and the larger peak currents for the two species are obtained in pH=7.0 (Fig. 5). Thus, this physiological pH [31] was chosen for the rest of the following measurements. The dependence of the peak potential of DA and AA on solution pH is linear with slope 51 mV per pH and 38.7 mV, respectively. For DA, the slope is nearly closed to the theoretical value of 59 mV per pH expected from the Nernst equation [32]. These values points that the overall process of two species contains equal number of protons and electrons. DA is oxidized to dopaminechrome [33] and AA is oxidized to dehydroascorbic acid [34], represented in (Scheme 1).

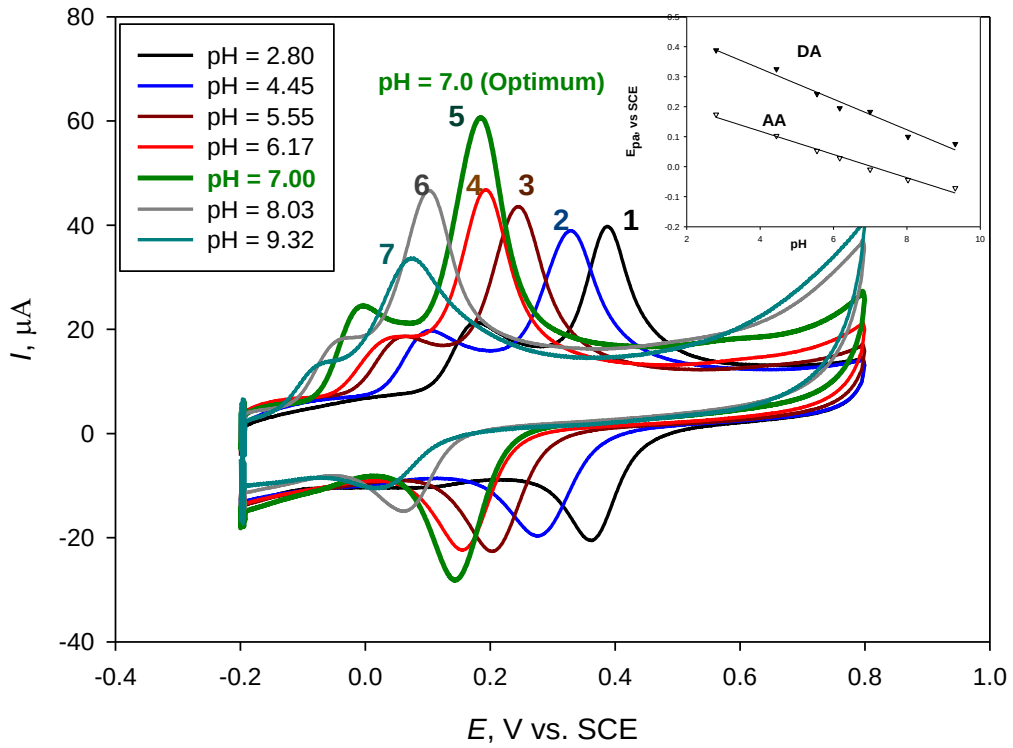

Figure 5. CVs obtained at GC/NiO_x-Au electrode in PBs containing 0.25 mM DA + 1.0 mM AA. pH: (1) 2.80, (2) 4.45, (3) 5.55, (4) 6.17, (5) 7.0, (6) 8.03 and (7) 9.32. Scan rate 100 mV s^{-1}. Inset: Dependence of the anodic peak on pH value of the solution.

3.4. Selectivity response of DA in the presence of AA.

The selectivity of the electroanalysis for DA and AA was investigated by measuring the CVs at the GC/NiO_x-Au electrode for 1 mM AA in the presence of different concentrations of DA as shown in Fig. 6. The DA oxidation peak increases while the oxidation peak of AA remains constant, points to the possible selective simultaneous analysis of the two species in their coexistence.

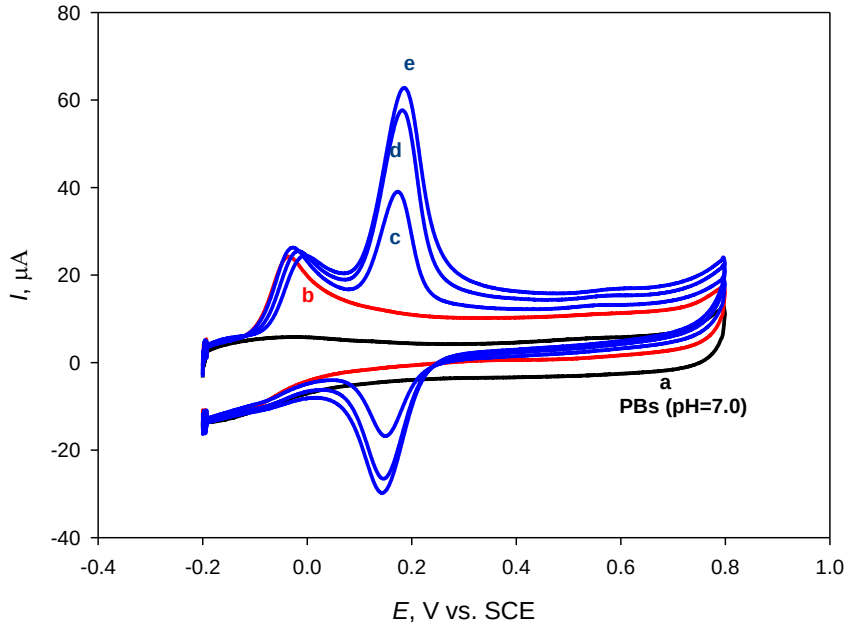

Figure 6. CVs obtained at GC/NiO_x-Au electrode in (a) PBs (pH=7.0) containing (b) 1.0 mM AA and (c, d, e) 1.0 mM AA and different concentrations of DA: (c) 0.125, (d) 0.25, (e) 0.375 mM. Scan rate 100 mV s^{-1}.

3.5. Effect of Scan Rate (SR).

The effect of scan rate on the electrochemical response of DA and AA at GC/NiO_x-Au was examined (Fig. 7). As shown in (Fig. 7 A and B), the peak currents of the two species regularly increased with the scan rate**.**

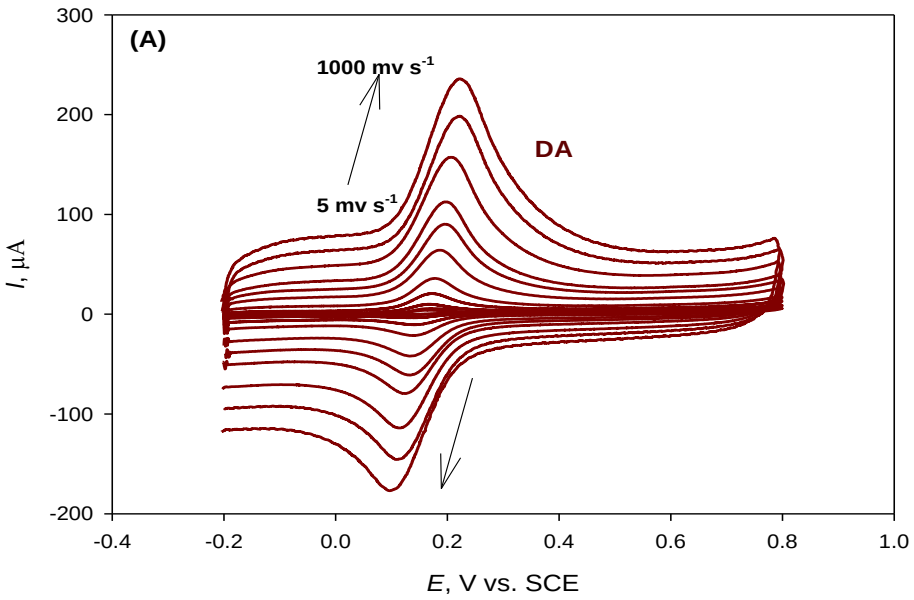

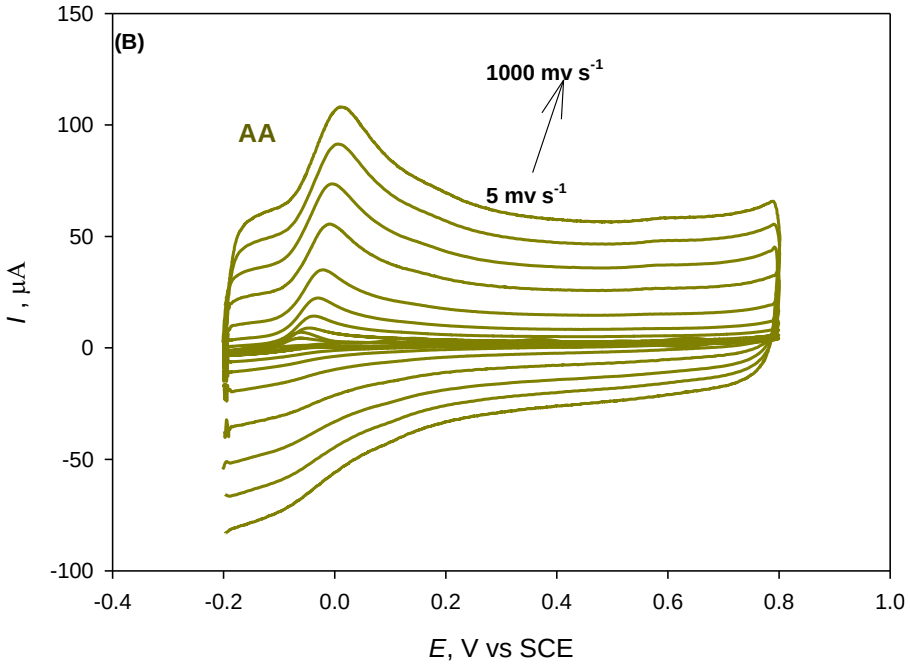

Figure 7. CVs of (A) 0.25 mM of DA and (B) 1 mM AA at GC/NiO_x-Au electrode in 0.1 M PBs (pH 7.0) at various scan rate :5, 10, 20, 50, 100, 200, 400, 600, 800 and 1000 mV s^{-1}.

The plot of oxidation peak current versus the square root of scan rate ($\nu^{0.5}$) (Fig. 8B), yields a straight line for AA, which suggests that the oxidation of AA at GC/NiO_x-Au to be diffusion controlled [35], but for DA the relation is not linear (Fig.8A).

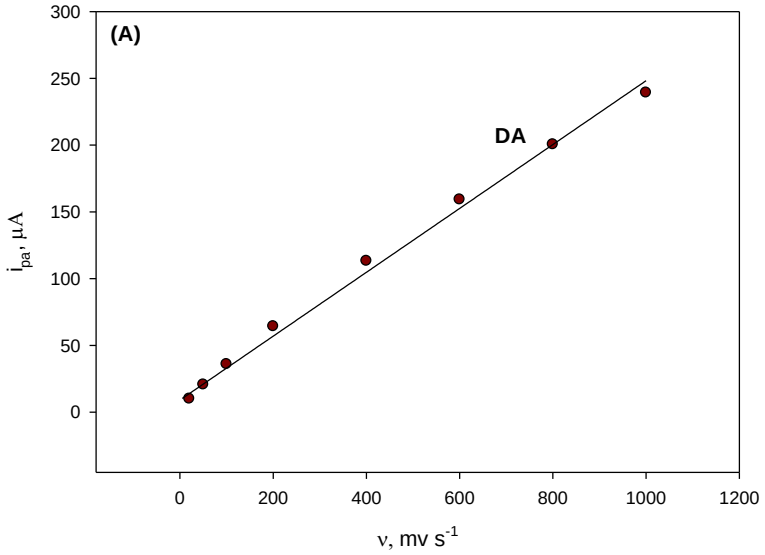

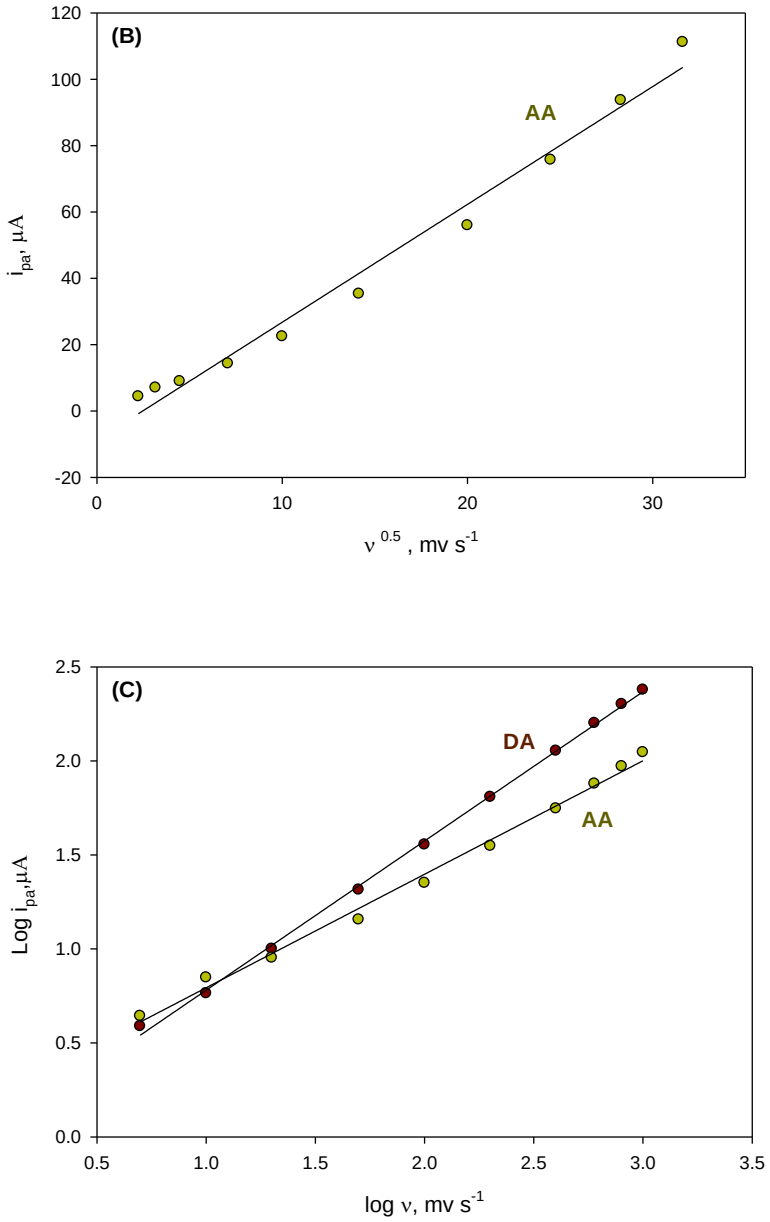

Figure 8. (A) $i_{pa} - \nu$ plot, (B) $i_{pa} - \nu^{0.5}$ plot and (C) Log i_{pa} – log ν plot for DA and AA at GC/NiO_x - Au electrode.

For DA, the linear relation is obtained between the oxidation peak current and *v* indicating that electrochemical process is surface controlled. In (Fig. 8C) a linear response of anodic peak current versus scan rate (log i_{pa} - log *v* plot) was also obtained. The slope of the log i_{pa} versus log *v* is calculated to be 0.79 (R^2 = 0.999) for DA and 0.60 (R^2 = 0.993) for AA. According to literature [36], the slope of DA 0.79 is nearly close to the theoretical value of 1 for adsorption – controlled processes. Also, the slope of AA 0.60 indicates that diffusion-controlled process occurs at GC/NiO_x-Au electrode.

3.6. Effect of Concentration.

Fig. 9. Shows CVs obtained at the surface of GC/NiO_x-Au electrode in the presence of different concentrations of DA and AA, [DA]: (0.125, 0.25, 0.375, 0.5, 0.625, 0.75 and 0.875 mM) and [AA]= 4 [DA] at scan rate was 100mVs^{-1}. The oxidation peaks of DA and AA increased regularly with increasing their concentrations. However, the two peaks tend to overlap with increasing the concentration of the two species. Thus, square wave voltammetric measurements were conducted, see below. The analytical plot (Fig. 9, inset) for voltammetric determination of DA and AA are linear in the range of 0.125–0.875 mM and 0.5–3.5 mM of DA and AA concentration, respectively. A correlation coefficient (R^2) of DA is 0.994 and 0.995 for AA**.**

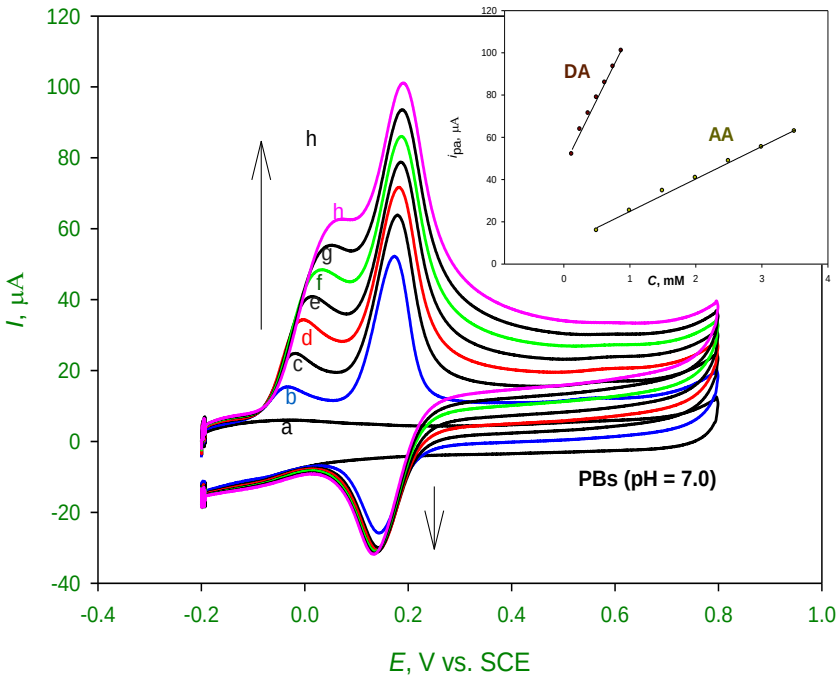

Figure 9. CVs obtained at different concentrations of DA and AA at the GC/NiO_x-Au electrode in 0.1 M Na_2HPO_4 PBs (pH 7.0). Scan rate: 100mVs^{-1}. [DA]: (0.125, 0.25, 0.375, 0.5, 0.625, 0.75 and 0.875 mM) and (a) 0.0 mM DA + 0.0 mM AA, (b) 0.125 mM DA + 0.5 mM AA, (c) 0.25 mM DA + 1.0 mM AA, (d) 0.375 mM DA + 1.5 mM AA, (e) 0.5 mM DA + 2.0 mM AA and (f) 0.625 mM DA + 2.5 mM AA, (g) 0.75 mM DA + 3.0 mM AA and (h) 0.875 mM DA + 3.5 mM AA. Inset: calibration curve of DA and AA.

3.7. Square Wave Voltammetry (SWV).

Square wave voltammetry (SWV) offers immunity against double-layer charging current and accordingly it is of high sensitivity compared with cyclic voltammetry [37]. The SWVs of both species in their coexistence were conducted at GC/NiO_x-Au electrode and results are shown in Fig. 10 in which the regular increase in the two peaks with the concentration of the two species is shown. The oxidation

peaks of DA and AA are noticeably detected at about 0.15 and - 0.04 V, respectively. What's more, that modified electrode exhibited the larger response for the oxidation of DA compared to AA and the AA had no interference for the determination of DA. Based on the SWVs obtained, the calibration curves for the two species are obtained and shown as inset. It seems that there are two regions with two different slopes for the calibration curves of the two species. While, AA shows linear relations within studied range, DA response tend to plateau at concentration larger than 0.028 mM.

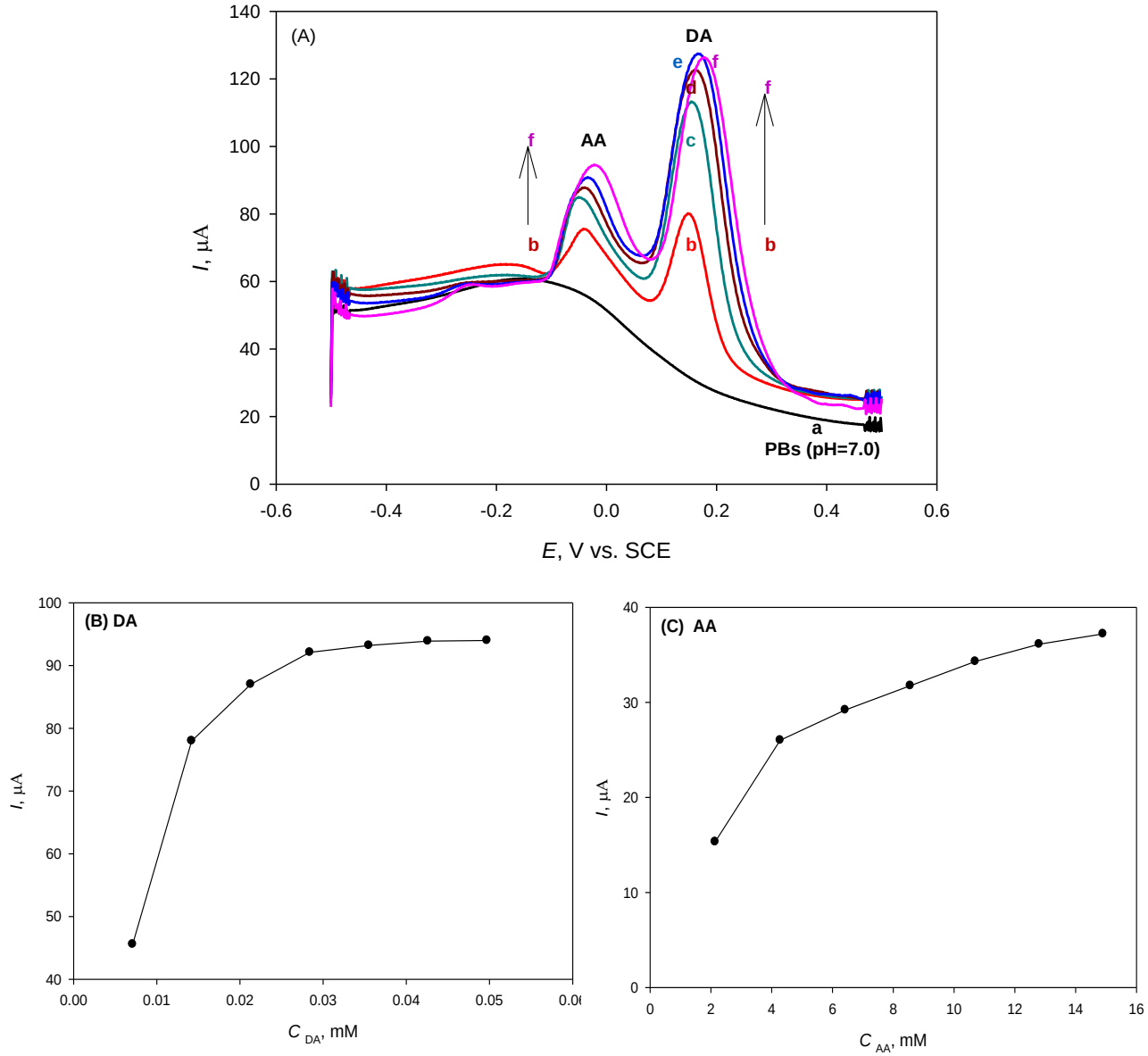

Figure 10. SWVs obtained at GC/NiO_x-Au electrode in (a) PBs (pH 7.0) containing different concentrations of DA and AA: (b) 0.007 mM DA + 2.14 mM AA, (c) 0.014 mM DA + 4.28 mM AA, (d) 0.021 mM DA + 6.42 mM AA, (e) 0.028 mM DA + 8.56 mM AA and (f) 0.035 mM DA + 0.011 mM AA. Square wave amplitude: 25 mV; frequency: 25 Hz; step potential: 2 mV. The electrode potential was scanned from –0.5 V to 0.5 V. (B) Calibration curve of peak current vs. concentration of DA. (C) Calibration curve of peak current vs. concentration of AA.

Table 2. Parameters of the electroanalytical determination of DA and AA using SWV.

Parameter	**DA**	**AA**
Optimum buffer	Phosphate	Phosphate
Optimum pH	7.00	7.00
Measured potential, (mV)	150	- 40
Scan rate, (mVs^{-1})	100	100
Linear concentration range, (μM)	7.1 – 49.7	2140 – 14900
Slope, ($\mu A\ cm^{-2}/\mu M$)	13.171	0.021
Correlation coefficient, R^2	0.869	0.929
Standard deviation, SD (n = 7), (mM)	0.007	0.105
Relative standard deviation, %	1.89	0.34
LOD, (μM)	0.079	15
LOQ, (μM)	0.265	51

Table 3. Comparison of analytical parameters for the detection of DA and AA at GC/NiO_x-Au with other modified electrodes.

Materials	**Technique**	**Analyte**	**Linear Range** (μM)	**LOD** (μM)	**Reference**
Au-RGO/GCE [a]	DPV	DA	6.8–41	1.4	[39]
		AA	240–1500	51	
Au-AGR-MWCNT/GCE[b]	SWV	DA	1.0–210	0.08	[40]
		AA	10–150	0.27	
AuNPs-β-CD-Gra/GCE [c]	SWV	DA	0.5–150	0.15	[41]
		AA	30–2000	10	
Au–Pd–GC electrode [d]	CV	DA	0.1-1000	0.08	[42]
		AA	1-5000	0.60	
GC/NiO_x-Au	SWV	DA	7.1 – 49.7	0.079	**This work**
		AA	2140 - 14900	15	

[a](Au nanoplates and reduced graphene oxide (RGO) modified glassy carbon electrode (GCE)), [b](gold nanoclusters (Au)/activated graphene (AGR)/MWCNT nanocomposite),[c](gold nanoparticles–cyclodextrin–graphene-modified electrode), [d](glassy-carbon electrode modified with binary systems based on gold, palladium, and rhodium).

The LOD and LOQ for DA were calculated as 0.079 and 0.265 μM, respectively and for AA as 15 and 51 μM, respectively. The LOD and LOQ were calculated from the calibration curve using the equation (LOD =3 *SD*/*N*) and (LOQ = 10 *SD*/*N*), where *SD* is standard deviation and *N* is the slope of the regression line [38]. Relevant parameters for the analysis of DA and AA at the GC/NiO_x-Au electrode are summarized in Table 2**.** The comparison of this method with other reported electrochemical methods

are given in Table 3. It can be seen that the GC/NiO_x-Au exhibited a wider linear range with lower detection limit of DA in comparison with other relevant reported results.

3.8. Study of Interferences.

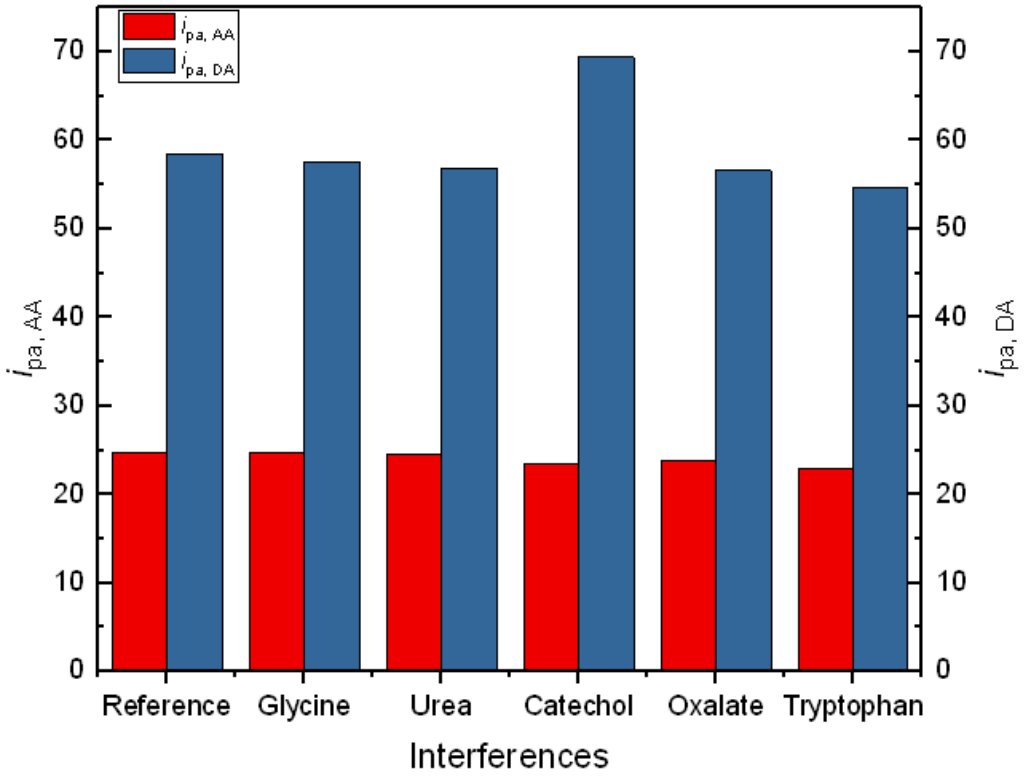

Figure 11. Effect of interferences on DA and AA detection. The concentration of DA, AA, tryptophan and other interferences is 0.25 mM, 1 mM, 0.05mM and 0.50 mM, respectively.

It is an important factor for a modified electrode to discriminate the similar interfering species to the target analytes. The influences of some possible interfering species in the analysis of DA and AA at GC/NiO_x-Au modified electrode is examined. Various interfering chemicals including amino acids (glycine and tryptophan), urea, oxalate and catechol were added to sample solutions in the presence of 0.25 mM DA and 1 mM AA. As can be seen in Fig.11, i_{pa} in the absence (Reference) of the interferences and in the presence of glycine, urea, potassium oxalate and tryptophan, are almost the same, It is noteworthy to mention that catechol increase the peak current of DA compared with other substances, which could be attributed to its similar structure as to DA. DA is a type of catecholamine 3,4-dihydroxyphenyl (catechol) [43].

4. CONSLUSIONS

The GC/ NiO_x-Au electrode has obvious advantage of simultaneously detection of DA in the presence of an excess of AA at the physiological pH (7.0). The modified electrode presented high

selectivity and sensitivity towards the oxidation of DA and AA. Thus the modified electrode successfully resolved the overlapped single anodic peak, obtained at the bare electrode, of the analytes into two distinct peaks, and thus DA can be detected selectively in the presence of excess of AA. This proposed electrode resulted an acceptable detection limit, higher sensitivity and selectivity of DA, even in the presence of a 10 to 100-fold excess of AA.

ACKNOWLEDGEMENTS
The Authors would like to thank the Deanship of Scientific Research at Umm Al-Qura University for supporting this work by Grant Code: 18-SCI-5-06-0003.

References

1. S. E. Hyman and R. C. Malenka, *Nat. Rev. Neurosci*., 2 (2001) 695.
2. R. M. Wightman, L. J. May and A. C. Michael, *Anal. Chem*., 60 (1988) 769A.
3. R. K. Shervedani, S. M. Siadat-Barzoki and M. Bagherzadeh, *Electroanalysis*, 22 (2010) 969.
4. C. J. Watson, B. J. Venton and R. T. Kennedy, *Anal. Chem.*, 78 (2006)1391.
5. J. Chen and C. S. Cha, *J. Electroanal. Chem.*, 463 (1999) 93.
6. S. Zhu, H. Li, W. Niu and G. Xu, *Biosens. Bioelectron.*, 25 (2009) 940.
7. D. Amin, *Analyst*, 111 (1986) 255.
8. N. Shafi, J. M. Midgley, D. G. Watson, G. A. Smail and R. Strang, *J. Chromatogr*., 490(1989) 9.
9. F. B. Salem, *Talanta*, 34 (1987) 810.
10. P. Kumarathasan and R. Vincent, *J. Chromatogr. A*., 987 (2003) 349.
11. G. H. Ragab, H. Nohta and K. Zaitsu, *Anal. Chim. Acta*, 403 (2000)155.
12. T. Zetterstrom, T. Sharp, C. A. Marsden and U. Ungerstedt, *J. Neurochem.*, 41 (1983) 1769.
13. P. Shakkthivel and S. M. Chen, *Biosens. Bioelectron.*, 8 (2007) 1680.
14. A. I. Gopalan, K. P. Lee, K. M. Manesh, P. Santhosh, J. H. Kim and J. S. Kang, *Talanta*, 4 (2007) 1774.
15. B. Fang, G. Wang, W. Zhang, M. Li and X. Kan, *Electroanalysis*, 9 (2005) 744.
16. J. Chen, J. Zhang, X. Lin, H. Wan and S. Zhang, *Electroanalysis*, 5 (2007) 612.
17. S. Y. Yi, H. Y. Chang, H. H. Cho, Y. C. Park, S. H. Lee and Z. U. Bae, *J. Electroanal. Chem.*, 2 (2007) 217.
18. N. West, P. Baker, T. Waryo, F. R. Ngece, E. Q. Iwuoha, C. Sullivan and I. Karakis, *J. Bioact. Compat. Polym.*, 28 (2013) 167.
19. A. R. Halpern, N. Nishi, J. Wen, F. Yang, C. Xiang, R. M. Penner and R. M. Corn, *Anal. Chem*., 81 (2009) 5585.
20. A. Salimi, R. Hallaj and S. Soltanian, *Electroanalysis*, 21 (2009) 2693.
21. C. Li, Y. Liu, L. Li, Z. Du, S. Xu, M. Zhang, X. Yin and T. Wang, *Talanta*, 77 (2008) 455.
22. M.I. Awad, B.A.AL Jahdaly, M. A. Kassem and O. A. Hazazi, *J. Anal. Chem*., 73 (2018) 1188.
23. H. Liu, X. L. Wu, B. Yang, Z. J. Li, L. C. Lei and X. W. Zhang, *Electrochim. Acta*, 174 (2015) 745.
24. M. I. Awad, M. A. Kassem, A. M. Hameed, B. A. Al Jahdali and O. A. Hazazi, *Orient. J. Chem*., 33 (2017) 1767.
25. M. Moharana and A. Mallik, *Electrochim. Acta*, 98 (2013) 1.
26. H. Shang, Y. Lu, F. Zhao, C. Chao, B. Zhang and H. Zhang, *RSC Adv*., 5 (2015) 75728.
27. S. J. Li, N. Xia, X. L. Lv, M. M. Zhao, B. Q. Yuan and H. Pang, *Sens. Actuators, B*, 190 (2014) 809.
28. W. Wang, H. Y. Wang, W. Wei, Z. G. Xiao and Y. Wan, *Chem. Eur. J*., 17 (2011) 13461.
29. N. Nordin, N. A. Yusof, S. Radu and R. Hushiarian, *J. Visualized Exp.*,136 (2018)1.
30. H. Bagheri, A. Afkhami, P. Hashemi and M. Ghanei, *RSC Adv*., 5 (2015) 21659.
31. T. M. Nancy, V. Anithakumary and B. K. Swamy, *J. Electroanal. Chem*., 720 (2014)107.

32. T. Hizawa, K. Sawada, H. Takao and M. Ishida, *Jpn. J. Appl. Phys.*, 45 (2006) 9259.
33. S. Saeed and B. Somayeh, *Electrochim. Acta*, 51 (2006) 4271.
34. J. C. Deutsch, *J. Chromatogr. A*, 881 (2000) 299.
35. A. Mohammadi, A. B. Moghaddam and J. Badraghi, *Anal. Methods*, 4 (2012) 1024.
36. K. B. E. Swamy and P. S. Ganesh, *J. Electroanal. Chem.,* 19 (2015) 752.
37. A. Babaei, M. Aminikhah and A. R. Taheri, *Sens. lett*., 11 (2013) 413.
38. T. Huang, Z. He, B. Yang, L. Shao, X. Zheng and G. Duan, *J. Pharm. Biomed. Anal*., 41 (2006) 644.
39. C. Wang, J. Du, H. Wang, C. Zou, F. Jiang, P. Yang and Y. Du, *Sens. Actuators, B,* 204 (2014) 302.
40. A.A. Abdelwahab and Y. Shim, *Sens. Actuators, B*, 221 (2015) 659.
41. X. Tian, C. Cheng, H. Yuan, J. Du, D. Xiao, S. Xie and M. M. Choi, *Talanta*, 93 (2012) 79.
42. L. G. Shaidarova, I. A. Chelnokova, A. V. Gedmina and G. K. Budnikov, *J. Anal. Chem*., 64 (2009) 36.
43. Z. Pourghobadi and D. Neamatollahi, *J. Serb. Chem. Soc.*, 82 (2017) 1053.